World Journal of Surgical Oncology

RESEARCH

Open Access

Three-dimensional and magnified CT images of displaying the imaging features of invasive adenocarcinoma of lung

Jincheng Chi[1], Wenxue Wu[1], Hua Zhong[1*] and Shaoyin Duan[1*]

Abstract

Objective To discuss CT imaging characteristics of invasive adenocarcinoma of lung(IACL).

Methods CT revealed the nodule of lung which pathology confirmed as IACL of 290 cases. Imaging data were retrospectively analyzed by dividing into high-risk group of 115 cases and low-risk group of 175. Three dimensional (3D) and magnified technology were used to show the nodules, which were observed and measured. Data of density, size and location of nodule were collected, and T-test or Chi-square test were performed.

Results In 290 cases with IACL, all lesions appeared as nodule with lobulated and vascular/cord shadows, which can be clearly shown by the 3D and magnified images. 153 (52.8%) were solid nodule, 43 (14.8%) sub-solid, 29 (10.0%) ground glass and 65 (22.4%) nodule with cavity or vacuole. Nodules less than 1 cm were in 19 cases (6.5%), 1–2 cm in 180 (62.1%) and 2–3 cm in 91(31.4%).Nodules with spherical growth were in 109 cases (37.6%), non spherical growth in 181 (62.4%). Nodules with equal or less than four vascular/cord shadows were in 61 cases (21.1%) and more than four in 229 (78.9%). There are significant differences between high-risk and low-risk groups in density, size, and vascular/cord shadows ($P<0.05$), no significant difference in nodule location and growth direction ($P>0.05$).The growth angle were shown to be 45 ° or 135 ° in 144 (79.6%)cases, there was significant difference in the growth angle of sagittal plane between on the right and left ($P=0.032$).

Conclusion Magnified and 3D technology can clearly show the features of IACL, which are lobulated nodule with vascular/cord shadows, and the most are solid nodule. Nodule with cavity or vacuole and less than 2 cm more appear in low-risk group. Growth angle may reflect the growth pattern of IAC and the pathological characteristics.

Keywords Lung adenocarcinoma, High and low risk, CT image, Growth mode and direction

*Correspondence:
Hua Zhong
281905583@qq.com
Shaoyin Duan
xmdsy@xmu.edu.cn
[1]Department of Radiology, School of Medicine, Zhongshan Hospital of Xiamen University, Xiamen University, Xiamen, China

Lung cancer is one of the most common malignant tumors in the world, and its mortality rate ranks first among malignant tumors. Lung adenocarcinoma is type of non-small cell cancer and originates from bronchial mucosal epithelium and mucous glands. Its incidence rate has replaced that of squamous cell carcinoma as the first histological type of lung cancer in China [1–4]. In the International Association for the Study of Lung Cancer (IASLC), American Thoracic Society (ATS) and European Respiratory Society (ERS) jointly developed the International Multidisciplinary New Classification of Lung Adenocarcinoma (LAC) in 2011, invasive adenocarcinoma of lung (IACL) was classified into five subtypes: acinar, adherent, papillary, micropapillary and solid dominant (New classification of lung adenocarcinoma: when the proportion of micropapillary components in the tumor exceeds 5%, it is defined as micropapillary type. For other types, all growth patterns of invasive lung adenocarcinoma in the observation field are recorded in increments of 5%. Finally, the growth pattern with the highest percentage is defined as the main pathological subtype of LAC) [5, 6]. Researchers have revealed that patients with IACL mainly composed of micropapillary or solid structures have poor survival prognosis and higher recurrence rates [7–10]. In this article, the IACL were divided into high-risk group including micropapillary or solid structures, and low-risk group including acinar, adherent and papillary structures. The relevant imaging features were discussed.

Materials and methods

Research subjects

290 patients with postoperative pathological diagnosis of IACL were collected, who underwent chest CT examination in our hospital from October 2018 to October 2023, their data of CT images were retrospectively analyzed. Inclusion criteria: ① Preoperative chest CT with plain scan and enhanced scan; ② The maximum diameter of single pulmonary nodule (≤ 30 mm) measured on CT image; ③ Postoperative pathological diagnosis of IACL; ④ Complete pathological data. Exclusion criteria: ① Poor CT image quality; ② Patients with unclear pathological subtype; ③ Multiple nodules in the lungs or recurrent nodules after surgery. Among 290 patients, there were 136 males and 154 females, with an age range of 25–86 years and a mean of 60.3 ± 10.1 years. Two groups were divided according to pathological subtypes, one was the high-risk with 115 cases including 102 of micropapillary type and 13 of solid type, the other was the low risk group with 175 cases including 142 of acinar type, 18 of adherent type and 15 of papillary type.

Equipment and methods

CT scanning equipment included the IQon spectral CT, Ingenuity spiral CT and Flash dual-source CT. The patient was on supine position and both of hands raised and held on his head. The scan was performed after holding the breath at the end of deep inhalation. Scanning range: from the entrance of the chest to the bottom of the lungs. Scanning parameters: collimator of 0.625 mm, pitch of 1.2 mm, tube voltage of 120 KV with the automatic adjustment of tube current, matrix size of 512 × 512, image thickness of 1.25 mm. All patients underwent plain CT and enhanced scan by injecting 70 ml of Levofloxacin (containing 300 mg/ml iodine, Bayer) through the elbow vein at rate of 3.0 ml/s, and CT arterial and venous phase images were obtained with delays of 25s and 60s, respectively.

Image processing and data analysis

A research group of three radiologists (one of whom was the senior physician, used the unified and standardized 3D image processing techniques and nodule measurement methods to minimize perceived differences. There are uncertain situations that need to be discussed and completed by three radiologists together) performed the image processing and data collection: ① selected the images of CT plain scan, arterial phase and venous phase of patients with IACL; ② uploaded the selected images to 3D image workstation, the lesion were observed and displayed by 3D imaging in the cross-sectional, sagittal and coronal planes; ③ the local image of lesion was magnified as the same proportion and set the same window level and width(-200,1500); ④ the lesion was observed and measured (Figs. 1 and 2), including the location, density and size of lesion, and the vascular/cord shadows (equal or less than four and more than four), pleural indentation sign, growth mode (the spherical or no-spherical growth), growth direction (in the cross-sectional, sagittal and coronal plane) and growth angle (composed of the longest diameter of lesion and the horizontal line. A°=0 indicated $-22.5 < A° < 22.5$, A°=45 indicated 22.5–67.5, A°=90 indicated $67.5 < A° < 112.5$ and A°=135 indicated 112.5-157.5). These data were statistical analyzed by t-test or chi-square test, $P < 0.05$ indicated the significant differences. All the study process see the flowchart (Fig. 3).

Result

1. General imaging features of IACL: In 290 patients with IACL, all lesions appeared as nodule with lobulated or irregular changes in the images of conventional CT and 3D imaging, which clearly showed all the signs with the magnified techn Fig. (Fig. 4). The image density of lesions was classified as the solid in 153 cases (52.8%), subsolid in 43 cases (14.8%), ground glass in 29 cases (10.0%), and nodule with cavity or vacuole in 65

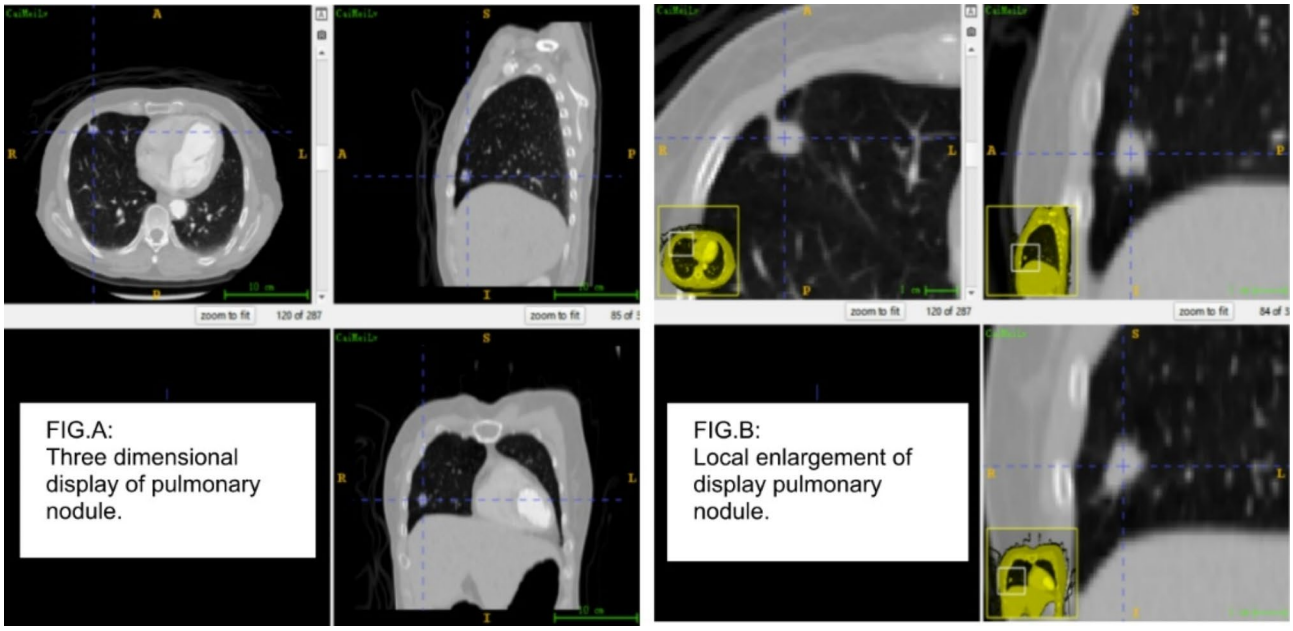

Fig. 1 A images showed the lesion by 3D images in the cross-sectional, sagittal and coronal planes; B images showed the lesion with the magnified technology

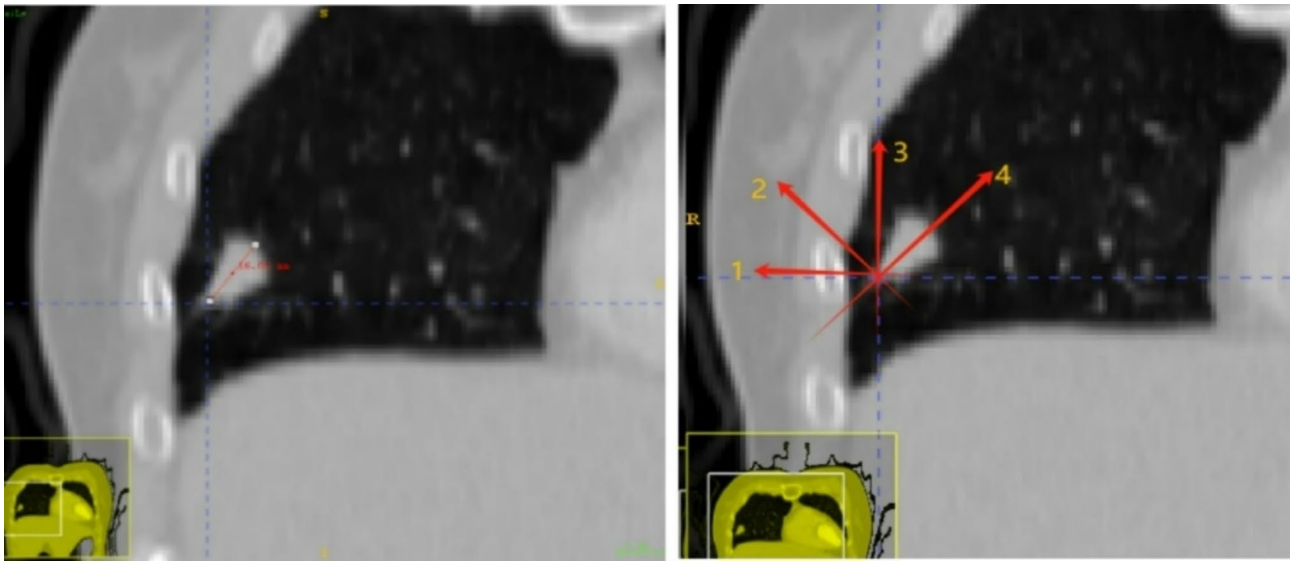

Fig. 2 The left image showed that the lung nodule with no-spherical growth and the longest diameter in the coronal plane with 16 mm. The right image shows the growth direction in the coronal plane and growth angle, which was composed of the longest diameter (4) and horizontal plane (1), and the growth angle was approximately 135°

cases (22.4%). The longest diameter of lesions was classified as the less than 1 cm in 19 cases (6.5%), more than or equal to 1 cm and less than or equal to 2 cm in 180 cases (62.1%), and more than 2 cm and less than 3 cm in 91 cases (31.4%). 260 cases (89.7%) showed bronchial or vacuole sign within the nodules, 109 cases (37.6%) were the spherical growth and 181 cases (62.4%) were the no-spherical. 61 cases were found the vascular/cord shadows around nodule ($\leqq 4$), 229 cases (78.9%) were found the vascular/cord shadows (>4). 173 cases (59.7%) were found the pleural indentation Fig. (Figures 5 and 6). There were significant differences in lesion density, size and vascular/cord shadows between the high and low-risk groups ($P<0.05$, Table 1).

2. No-spherical growth direction and angle: Among 181 cases with IACL of no-spherical growth, 52 cases (28.7%) showed growth direction in the cross section, 71 (39.2%) in the sagittal plane and 58 (32.1%) in the

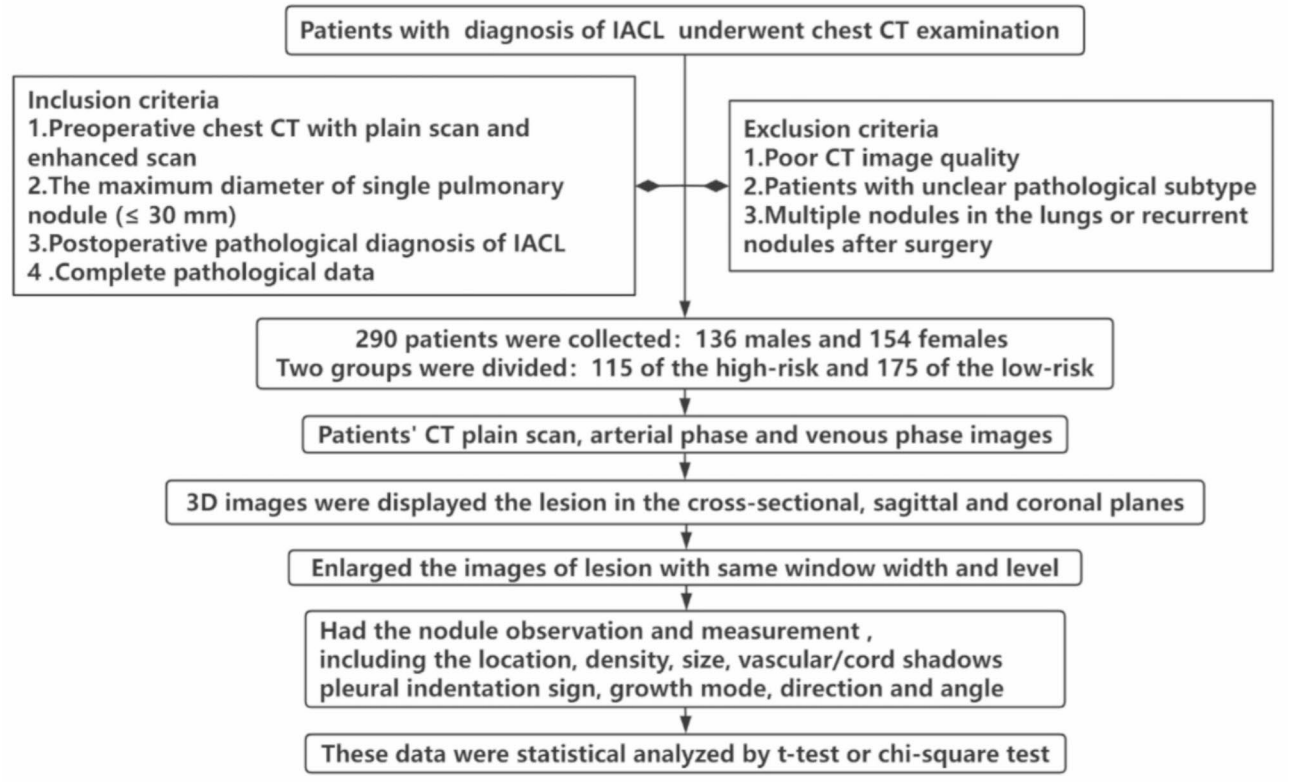

Fig. 3 The flow chart showed the whole research process and data processing

coronal plane. There were 86 (47.5%) cases on the left and 95 (52.5%) on the right. 67 cases (37.02%) were in the high-risk group and 114 (62.98%) in the low-risk group. There was no significant difference in the growth direction between the left and right, high and low risk groups ($P > 0.05$, Table 2). The growth angle were shown to be 45 ° in 81 cases (44.8%) and to be 135 ° in 63 cases (34.8%). There was significant difference in the growth angle of sagittal plane between on the right and left ($P = 0.032$), while no significant difference in the other growth angle ($P > 0.05$, Tables 2 and 3).

3. Growth pattern and location distribution: 109 cases of spherical growth were located in the lower lobe in 53 cases (48.6%), and in the upper lobe in 41 cases (37.6%). In the 181 cases of no-spherical growth, of which 52 cases of cross-sectional growth were located in the upper lobe in 30 cases (57.7%), 71 cases of sagittal growth were located in the upper lobe in 35 cases (49.3%) and 58 cases of coronal growth were located in the lower lobe in 38 cases (65.5%). In the 115 cases of high-risk group, lesions in the lower lobe accounted for 51 cases (44.3%), in the upper lobe 47 (40.9%); While in the 175 cases of low-risk group, in the lower lobe 74 cases (42.3%), in the upper lobe 72 (41.1%). No-spherical growth in the sagittal plane, lesions were on the right accounted for 43/71 cases (60.6%), on the left 28/71 (39.4%). Statistical analysis showed no significant difference in the lesion location between the left and right groups, as well as between the high-risk and low-risk groups ($P > 0.05$, Table 4).

Discuss

Imaging morphological characteristics of IACL

For the histological classification criteria, lung adenocarcinoma classify into three categories: pre-invasive, microinvasive and invasive adenocarcinoma (IACL). Among them, IACL is mainly divided into five pathological subtypes: acinar type, lepidic type, micropapillary type, papillary type and solid type. In this article divided them into the high and low-risk groups for related discussions, which is beneficial for improving the level of clinical imaging diagnosis and the selection of treatment plans [5, 6, 11–13]. The results of this study showed that the morphological characteristics of IACL that included ① the lesion appeares as nodule with lobulated or irregular shapes. ② the most is the solid nodule and the second is the cavity or vacuole within the nodule. ③ the nodules are mostly 1–2 cm in size. Some of these imaging features are consistent with literature reports, while the others have not been reported[1,2,]. There are statistically significant difference in lesion size between the high-risk and low-risk groups of IACL. The lesions of 1–2 cm in the

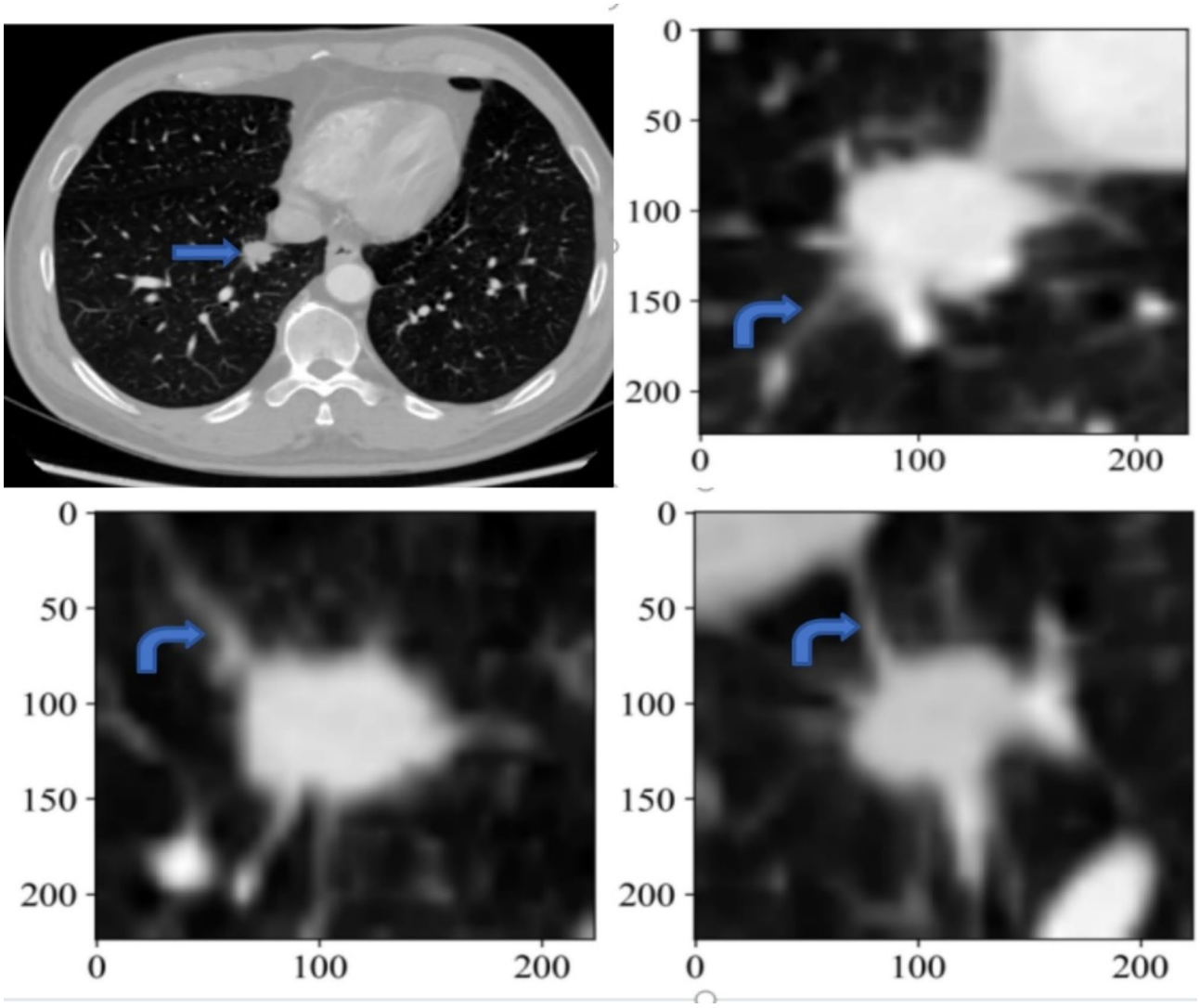

Fig. 4 The images of conventional CT(upper left, showing the lesion annotated by the straight arrow and 3D imaging (upper right in cross section, lower left in sagittal plane and lower right in coronal plane, clearly showing the lesion and vascular/cord shadows annotated by the curved arrow)

high-risk group are less than that in the low-risk group, while the lesions of 2–3 cm in the high-risk group are more than that in the low-risk group. This may be due to the relatively slow growth of lesion in the low-risk group and fast growth of lesion in the high-risk group, the relatively smaller size of IACL were discovered in the low-risk group, and the relatively larger one in the high-risk group. That reveal the pathological subtypes are closely related to tumor diameter [14–17]. The lobulated sign or irregularity of lesions present as the uneven arc-shaped or petal like appearance in the contour of lesion. It was found in the every lesion in the high- and low-risk groups of IACL without do the quantitative study which was a deficiency or regret. The formation reasons are the differential differentiation of tumor cells or the resistance from adjacent lung tissue, resulting in the tumor uneven growth. Our study found that the nodule was displayed more clearly and intuitively by CT three-dimensional imaging and magnification image than conventional image.

Imaging internal features of IACL

The internal features of lesion include the density, air bronchial shadow or vacuole within the nodule. This study found that these lesions were most commonly manifested as the solid nodules, which appeared more frequently in the high-risk group than in the low-risk group. Secondly, nodule with cavity or vacuole appeared more frequently in the low-risk group than in the high-risk group. In this article, authors used the new type of cavity within nodule, which can distinguish from the solid, sub-solid and ground glass nodule, and there are many cases in clinical practice. Of course, is the type necessary? which should be further more explorations

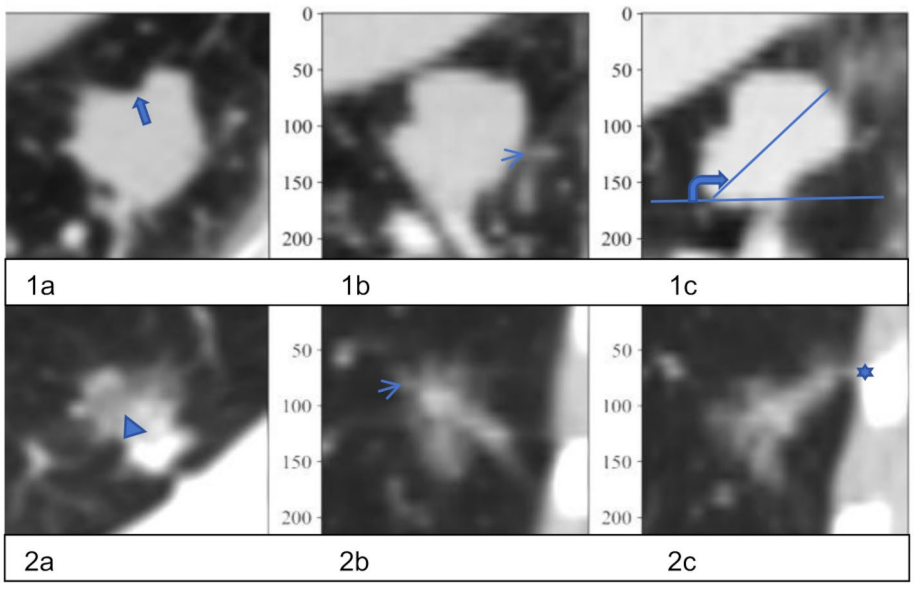

Fig. 5 High risk group patients of Case 1 (**1a**, **1b**, **1c**) and Case 2 (**2a**, **2b**, **2c**): Case 1 was the solid nodule with the lobulated sign (straight arrow in **1a**) and vascular/cord shadows (fine arrow in **1b**), with no-spherical growth in coronal plane and the growth angle of 135 °(curved arrow in **1c**). Case 2 was sub-solid nodule with no-spherical growth in cross section, with the irregular shape, bronchial shadow (arrow head in **2a**), vascular/cord shadows (fine arrow in Fig. **2b**) and pleural indentation sign (star in **2c**)

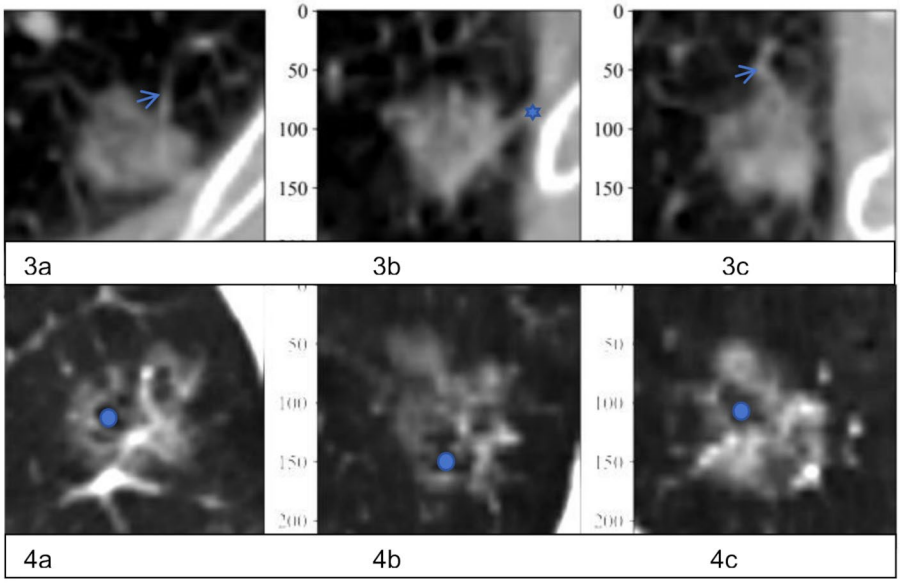

Fig. 6 Low risk group patients Case 3 (**3a**, **3b**, **3c**) and Case 4 (**4a**, **4b**, **4c**): Case 3 was the solid nodule with spherical growth, obvious lobulation sign, vascular/cord shadows (fine arrow in **3a**, **3c**) and pleural indentation sign (star in **3b**). Case 3 was the nodule with cavity or vacuole (round dot in **4a**, **4b**, **4c**), no-spherical growth in the coronal plane, vascular/cord shadows and the growth angle of 45°

and discussions. However, about the visual classification, it has the characteristics of simplicity and objectivity and is worthy of further research [16]. Air bronchial sign or vacuole sign is the appearance of strip or small air shadows in the lesion. This phenomenon is caused by the growth of tumor cells attached to the bronchial wall and bronchial lumen was been preservation. It's also possible for that the residual lung tissue has not been filled or destroyed by tumor tissue. Researchers have reported that the bronchial or vacuole sign is mainly seen in the lepidic adenocarcinoma with the well differentiation, which has relatively weak invasion ability and its

Table 1 CT imaging features of 290 cases of invasive lung adenocarcinoma

Groups		High Risk(115)	Low Risk(175)	X^2	*P*
Density	Solid	80	73	27.21	**0.000***
	Sub-solid	16	27		
	ground glass	9	20		
	With cavity or vacuole	10	55		
Size	< 1	3	16	7.663	**0.022***
	1 ≦ A ≦ 2	68	112		
	2 < A < 3	44	47		
Bronchial/ vacuole signs	yes	102	158	0.189	0.664
	no	13	17		
Growth mode and direction	Spherical	48	61	3.257	0.355
	Cross section	22	30		
	Sagittal plane	22	49		
	Coronal plane	23	35		
Vascular/ cord shadows	≦ 4	37	24	14.24	**0.000***
	> 4	78	151		
Pleural indentation sign	yes	76	97	3.276	0.070
	no	39	78		

* $P < 0.05$

Table 2 Comparison of no-spherical growth direction of 181 cases with IACL

Groups	Left	Right	High risk group	Low risk group
Cross section	29	23	22	30
Sagittal plane	30	41	22	49
Coronal plane	27	31	23	35
X^2	2.230		1.905	
P	0.328		0.386	

biological behavior usually manifests as low-grade malignancy [17, 18]. However, our result does not support this viewpoint, because there was no significant statistical difference in the occurrence of the bronchial or vacuole sign between the high-risk and low-risk groups, that require further studies for verification.

The related characteristics of growth pattern and direction of IACL

The imaging signs of lung adenocarcinoma are complex and diverse, IACL are often discovered by physical examinations or accidental discovery because of the other disease examinations. Making qualitative diagnosis of IACL is difficult. Clinical diagnosis often relies on pathological diagnosis from the surgery or puncture. CT imaging is a valuable application technology, but there have been no relevant reports on observing the adenocarcinoma growth mode and evolution process by CT. Our study found that IACL growth direction was spherical in 109 cases (37.6%) and no-spherical in 181 cases (62.4%), The no-spherical growth is the more common than the spherical. This also reflects the characteristic of uneven growth of adenocarcinoma and high degree of malignancy [15, 16]. Of course, the spherical growth is relative and local imbalances of lesion must be found. No-spherical growth can be in the directions of cross-sectional, sagittal and coronal planes, there were 67 cases (37.02%) in the high-risk group and 114 cases (62.98%) in the low-risk group, it indicates a higher incidence of no-spherical growth in the low-risk group, but there was no statistically significant difference in the growth direction between the left and right, high- and low-risk groups. The growth angles were more found at 45 ° and 135 °(79.6%). The explanation for this result may be that the lesion grows along the long axis of the bronchioles, but further data confirmation and proof are needed for this inference. Statistical analysis showed that there was significant difference in

Table 3 Comparison of growth angle of 181 cases between the left and right/the high and low risk group

Groups		Left				Right				X^2	P
		H-Risk36	L-Risk 50	X^2	P	H-Risk31	L-Risk64	X^2	P		
Cross section	0°	0	0	1.888	0.540	0	0	0.549	1.000	3.047	0.228
	45°	4	5			6	6				
	90°	1	5			2	3				
	135°	7	7			2	4				
Sagittal plane	0°	0	0	2.260	0.379	0	0	1.253	0.666	6.893	**0.032***
	45°	4	5			4	17				
	90°	3	8			1	5				
	135°	6	4			4	11				
Coronal plane	0°	0	2	2.702	0.555	0	0	0.660	0.874	2.384	0.295
	45°	7	6			6	11				
	90°	1	1			2	3				
	135°	3	7			4	4				

*$P < 0.05$, H-Risk = high risk groups, L-Risk = low risk groups

Table 4 Growth direction and location distribution of 290 cases with IACL

Groups and location (cases)		High Risk (115 cases)			Low Risk(175 cases)			X^2	P
		S_{1-3} (47)	S_{4-5} (17)	S_{6-10} (51)	S_{1-3} (72)	S_{4-5} (29)	S_{6-10} (74)		
spherical growth (109)	Left (52)	10	3	11	12	6	10	4.065	0.668
	Right (57)	8	2	14	11	4	18		
Cross section (52)	Left (26)	7	2	2	10	2	3	3.018	0.807
	Right (26)	4	3	4	9	2	4		
Sagittal plane* (71)	Left (28)	7	2	3	10	3	3	3.998	0.677
	Right (43)	3	2	5	15	8	10		
Coronal plane* (58)	Left (27)	2	2	7	1	2	13	8.017	0.237
	Right (31)	6	1	5	4	2	13		

* Added the compared pairwise between the four data of the sagittal and coronal planes, there all was no significant difference ($P > 0.05$)

growth angle of the sagittal plane between on the right and left. This implicate that there are certain differences in the growth angle of lung adenocarcinoma. About the growth direction and angle of IACL, at present, there are no any relevant report of literature, but the authors believe that are related to the growth pattern of IACL, which reflects the pathological characteristics [19, 20].

Distribution characteristics of IACL location

IACL is more common in the peripheral lung cancer, which occurs the segmental bronchus and the distal, and the lesion distribution has no obvious characteristics [15, 21]. Our results show that there are fewer lesions located in the middle lobe or tongue segment, which is not completely consistent with the reported by Li Yun et al. [21], who found that lesions appear more in the upper and middle lobes, and it is believed that may be related to the difference in the blood perfusion. The upper lung field has less blood perfusion, while the oxygen concentration in the alveolus is relatively high, which may be beneficial for the lesion growth. We found the nodule of spherical growth and coronal growth are mostly located in the lower lobe, while that of cross-sectional and sagittal growth are mostly located in the upper lobe. Nodule in the lower lobe accounted for 51/115 cases (44.3%) in the high-risk group, while 74/175 cases (42.3%) in the low-risk group, but statistical analysis showed no significant difference in the lesion distribution in lung between the left and right groups, as well as the high-risk and low-risk groups. Our results indicate that there is no differential diagnostic value from the lesion distribution of IACL, but authors found the more lesions in the upper and lower lobes.The reason for more lesions in the lower lobe may be related to smoking and air pollution, which the bronchi and alveoli in the lower lobe of lungs are more susceptible to harmful substances from tobacco or air. In addition, age and weakened immune system function can also lead to involvement of the lower lobe of the lungs [22, 23].

Peripheral features of IACL lesion

The peripheral features of IACL include the vascular/cord shadows and pleural indentation sign. Pleural indentation sign refers to the triangular or linear shadow between the tumor and pleura. Its pathological basis is fibrosis of the surrounding lung tissue and scar formation within the tumor, which affects and causes the pleural traction. The sign usually associated with the malignant biological behavior of the tumor [15, 21]. The vascular/cord shadows refers to the concentration of blood vessels or increased lymphatic vessels around lesion. The pathological basis is the abnormal thickening of blood or lymphatic vessels, and the traction from the fibrosis of lesion [17, 21]. Our results showed that vascular/cord shadows account for 100%, and more than 4 vascular/cord shadows for 78.9%. The signs are more in the low-risk group than the high-risk. The formation reasons of vascular/cord shadows are the thickening of bronchial vascular bundles and the dilation of small arteries and veins around the lesion, which can be seen in many diseases affecting blood vessels, bronchi, and fibrous connective tissue. However, different diseases have different characteristics, but it appears much more in malignant nodules than in benign nodules [21, 25–29]. The occurrence of pleural indentation sign was about 59.7%, and there was no difference between the high-risk group and the low-risk. The relevant literature reported [29–31] that pleural indentation sign and vascular/cord shadows can not reflect the different pathological subtype and cannot be used as the differential basis for the pathological subtypes. Then, our results showed the vascular/cord shadows present in IACL with the universal and characteristic, and rarely appears in benign nodule, it can become a sign of identifying benign and malignant nodule or the degree of differentiation of adenocarcinoma [26, 31]. This result can be related to the observation of 3D imaging and magnified image that have good ability to distinguish fine vessels, especially in the size measurements, external shape and internal density of lesion, and the counts of vascular/cord shadows and observing the

relationship between the lesion and surrounding structures [32, 33].

Study shortcomings and improvements

① The old standard of defined the subtypes of lung adenocarcinoma was used, the results certainly have certain shortcomings, but they also demonstrate good comparative value and propose a new research direction: the impact of new and old standards on CT imaging diagnosis and clinical prognosis [7, 34, 35].② The nodule classification was relying on subjective visual assessments, it should increase the other classification based on quantitative CTR (consolidation-to-tumor ratio) values and compare their differences.③ About the study on the relationship between CT imaging features and high-risk/low-risk lesions, it should increase the formation mechanism of imaging features and consider introducing predictive modeling techniques.④ This is a retrospective study and there may be data bias or missing data. The results should be interpreted with caution and further validated through prospective studies.⑤About the "No-spherical growth angle and Growth direction and location distribution", it need to expand the sample size and further conduct the statistical comparative research.

Conclusion

Overall, our results displayed that magnified image and 3D technology can clearly show the features of IACL, which are shown as the nodule with the lobulated or irregular, bronchial or vacuole sign and vascular/cord shadows. No-spherical growth are exceeding 50% and the growth angle of 45 ° and 135° are common. Most of nodule are the solid, the nodule with cavity or vacuole and less than 2 cm in low-risk group are more than the high-risk. Lower lobe lesions are more common in spherical growth and coronal growth, while upper lobe lesions are more in cross-sectional and sagittal growth.

Supplementary Information

The online version contains supplementary material available at https://doi.org/10.1186/s12957-025-03728-y.

Supplementary Material 1

Supplementary Material 2

Supplementary Material 3

Supplementary Material 4

Supplementary Material 5

Supplementary Material 6

Author contributions

Writing original draft: Jincheng Chi: Writing original draft and Data curation and prepared figuresShaoyin Duan: Writing original draft and Writing review & editing and Supervision and Project administration.Wenxue WU: Data curation and prepared figuresZhong Hua: Data curation and prepared figures and.

Funding statement

Project research supporting fund from zhongshan hospital of Xiamen University (KY-010507).

Data availability

No datasets were generated or analysed during the current study.

Declarations

Competing interests

The authors declare no competing interests.

Conflict of interest

The authors have no conflicts of interest to disclose.

Received: 4 November 2024 / Accepted: 25 February 2025
Published online: 10 March 2025

References

1. Respiratory Disease Branch of Chinese Medical Association. Consensus of Chinese experts on early lung cancer diagnosis (2023 edition) [J]. Chin J Tuberculosis Respiratory Dis. 2023;46(1):1–18. https://doi.org/10.3760/cma.j.cn112147-20220712-00592.
2. Li C, Lei SY, Ding L, et al. Global burden and trends of lung cancer incidence and mortality. Chin Med J. 2023;136:1583–90. https://doi.org/10.1097/CM9.
3. Siegel RL, Miller KD, Fuchs HE et al. Cancer statistics, 2022[J]. CA: A Cancer journal for clinicians,2022,72(1):7–33.
4. Cao W, Chen HD, Yu YW et al. Changing profiles of cancer burden worldwide and in China: a secondary analysis of the global cancer statistics 2020[J]. Chin Med J (Engl) 2021,134(7):783–91.
5. Gaillard F, Niknejad M, Elfeky M et al. Adenocarcinoma of the lung. Reference Article, Radiopaedia.org (Accessed on 28 Sep 2024). https://doi.org/10.53347/rID-22314
6. Warth A, Muley T, Meister M, et al. The novel histologic international association for the study of lung Cancer/American thoracic society/European respiratory society classification system of lung adenocarcinoma is a stage-independent predictor of survival[J]. J Clin Oncol. 2012;30(13):1438–46.
7. Travis WD, Brambilla E, Noguchi M, et al. International association for the study of lung Cancer/american thoracic Society/european respiratory society international multidisciplinary classification of lung adenocarcinoma[J]. J Thorac Oncol. 2011;6(2):244–85.
8. Zhao Y, Wang R, Shen X et al. Minor components of micropapillary and solid subtypes in lung adenocarcinoma are predictors of lymph node metastasis and poor Prognosis[J]. Ann Surg Oncol 2016,23(6):2099–105.
6. Miyoshi T, Satoh Y, Okumura S, et al. Early-stage lung adenocarcinomas with a micropapillary pattern, a distinct pathologic marker for a significantly poor prognosis. Am J Surg Pathol. 2003;27(1):101–9.
9. Zombori T, Nyari T, Tiszlavicz L, et al. The more the micropapillary pattern in stage I lung adenocarcinoma, the worse the prognosis-a retrospective study on digitalized slides. Virchows Arch. 2018;472(6):949–58.
10. Xu CW, Zhang B, WHO. (2015) histological classification of lung tumors [J]. Journal of Diagnostic Pathology, 2015, 22 (12): 815–816.
11. Pan Z, Hu G, Zhu Z et al. Predicting Invasiveness of Lung Adenocarcinoma at Chest CT with Deep Learning Ternary Classification Models. Radiology. 2024;311(1):e232057. 10.1148 /radiol.232057. PMID: 38591974.
12. Willner J, Narula N, Moreira AL. Updates on lung adenocarcinoma: invasive size, grading and STAS. Histopathology. 2024;84(1):6–17. https://doi.org/10.1111/his.15077. Epub 2023 Oct 23. PMID: 37872108.
13. Suster DI. Grading of invasive pulmonary adenocarcinoma: evolution of prior histologic classification systems to enhance lung cancer prognostication. Ann Diagn Pathol. 2024;71:152329. https://doi.org/10.1016/j.anndiagpath.2024.152329. Epub 2024 May 20. PMID: 38772118.
14. Rudinc M, Avila-Tang E, Harris CC, et al. Lung cancer in never smokers: molecular profiles and therapeutic implications [J]. Clin Cancer Res. 2009;15(18):5646–61.
15. Wang J, Mao XQ. Analysis of the relationship between CT signs and pathological subtypes, as well as the degree of tissue differentiation, in patients with peripheral lung adenocarcinoma [J]. Chin J Health Eng. 2024;23(04):540–2. https://doi.org/10.19937/j.issn.1671-4199.2024.04.036.

16. Chang YC, Chen PT, Hsieh MS, et al. Discrimination of invasive lung adenocarcinoma from Lung-RADS category 2 nonsolid nodules through visual assessment: a retrospective study. Eur Radiol. 2024;34(5):3453–61. https://doi.org/10.1007/s00330-023-10317-8. Epub 2023 Nov 2. PMID: 37914975.
17. Jin YF. Correlation between MSCT manifestations and pathological subtypes of peripheral invasive lung adenocarcinoma research on sexuality [D]. Qingdao: Qingdao University; 2017.
18. Hattori A, Suzuki K, Maejima T, et al. The presence of air bronchogram is a novel predictor of negative nodal involvement in radiologically pure-solid lung cancer. Eur J Cardiothorac Surg. 2014;45(4):699–702. https://doi.org/10.1093/ejcts/ezt467. Epub 2013 Oct 17.
19. Bai GY, Qiu B, Ji Y, et al. Progress in diagnosis and treatment of partial solid nodule lung adenocarcinoma on imaging manifestations [J]. Chin J Oncol. 2021;43(7):743–50.
20. Zhang C. Comparative analysis of CT imaging findings of isolated pulmonary solid nodules and pathological subtypes of lung adenocarcinoma. Imaging Res Med Appl. 2022;6(5):17–9.
21. Li Y, Jin YF, Bao S, et al. The correlation between the MSCT findings and the pathological subtypes of peripheral infiltrating lung adenocarcinoma [J]. Acad J Qingdao Univ (Medical Sciences). 2018;54(06):695–8.
22. Kinsey CM, Estepar RSJ, Zhao Y, et al. Invasive adenocarcinoma of the lung is associated with the upper lung regions[J]. Lung Cancer. 2014. https://doi.org/10.1016/j.lungcan.2014.02.002.
23. Lin YH, Hung JJ, Yeh YC, et al. Prognostic significance of basal versus superior segment in patients with completely resected lung adenocarcinoma in the lower lobe. Thorac Cancer. 2019;10(2):312–20. https://doi.org/10.1111/1759-7714.12957. Epub 2019 Jan 2. PMID: 30601596; PMCID: PMC6360222.
24. Allison DJ, Stanbrook H. 1979 George Simon memorial fellowsip award.a radiologic and physiologic investigation into hypoxic pulmonary vasoconstriction in the dog.invest radiol, 1980, 15(3):178–90.
25. Niu ZX, Zhou QH, Li X, et al. Non small cell lung cancer nodules on high-resolution CT research on changes in surrounding lung tissue and blood vessels. Chin J Lung Cancer. 2003;6(1):35–7.
26. Gao F, Li M, Ge X, Zheng X, Ren Q, Chen Y, et al. Multi-detectorspiral CT study of the relationships between pulmonary ground-glass nodules and blood vessels. Eur Radiol. 2013;23(12):3271–7. https://doi.org/10.1007/s00330-013-2954-3.
27. Liang J, Xu XQ, Xu H, Yuan M, Zhang W, Shi ZF, et al. Using the CT features to differentiate invasive pulmonary adenocarcinoma from pre-invasive lesion appearing as pureormixed ground-glass nodules. Br J Radiol. 2015;88(1053):20140811. https://doi.org/10.1259/bjr.20140811.
28. Zhang PJ, Li TR, Tao XM, et al. HRCT features between lepidic-predominant type and other pathological subtypes in early-stage invasive pulmonary adenocarcinoma appearing as a ground-glass nodule[J]. BMC Cancer. 2021;21(1):1124–1124.
29. Ko JP, Suh J, Ibidapo O, et al. Lung adenocarcinoma: correlation of quantitative CT findings with pathologic findings. Radiology. 2016;280(3):931–9. https://doi.org/10.1148/radiol.2016142975.
30. Liang J, Xu XQ, Xu H, et al. Using the CT features to differentiate invasive pulmonary adenocarcinoma from pre-invasive lesion appearing as pure or mixed ground-glass nodules. Br J Radiol. 2015;88(1053):20140811. https://doi.org/10.1259/bjr.20140811.
31. Xi RQ, Xie DH, Hu CH et al. The value of perinodular vascular concentration sign in the diagnosis of small lung cancer [J]. Chin J Med Imaging, 1998, (03): 178–80.
32. Gao F, Li M, Ge X, et al. Multi-detector spiral CT study of the relationships between pulmonary ground-glass nodules and blood vessels. Eur Radiol. 2013;23(12):3271–7. https://doi.org/10.1007/s00330-013-2954-3.
33. Gharraf SH, Mehana MS,,ElNagar AM. Role of CT in differentiation between subtypes of lung cancer; is it possible?[J]. Egypt J Bronchol 2020,14(1):1–7. https://doi.org/10.1186/s43168-020-00027-w
34. Yoshida Y, Nitadori JI, Shinozaki-Ushiku A, et al. Micropapillary histological subtype in lung adenocarcinoma of 2 cm or less: impact on recurrence and clinical predictors. Gen Thorac Cardiovasc Surg. 2017;65(5):273–9. https://doi.org/10.1007/s11748-017-0747-3. Epub 2017 Feb 27. PMID: 28243892.
35. Moreira AL, Ocampo PSS, Xia Y et al. A grading system for invasive pulmonary adenocarciioma: A proposal from the international association for the study of lung Cancer pathology committee.j thorac oncol. 2020,15(10): 1599–61010.1016 /j. jtho.2020.06.001

Publisher's note